In vivo terahertz imaging of rat skin burns

Priyamvada Tewari
Colin P. Kealey
David B. Bennett
Neha Bajwa
Kelli S. Barnett
Rahul S. Singh
Martin O. Culjat
Alexander Stojadinovic
Warren S. Grundfest
Zachary D. Taylor

In vivo terahertz imaging of rat skin burns

Priyamvada Tewari,[a] Colin P. Kealey,[b] David B. Bennett,[c]
Neha Bajwa,[a] Kelli S. Barnett,[d] Rahul S. Singh,[a,b]
Martin O. Culjat,[a,b] Alexander Stojadinovic,[e,f]
Warren S. Grundfest,[a,b,c] and Zachary D. Taylor[a]
[a]UCLA, Department of Bioengineering, Los Angeles, California 90095
[b]UCLA, Department of Surgery, Los Angeles, California 90095
[c]UCLA, Department of Electrical Engineering, Los Angeles, California 90095
[d]UCLA, Division of Laboratory Animal Medicine, Los Angeles, California 90095
[e]Walter Reed Army Medical Center, Combat Wound Initiative Program, Washington, DC 20307
[f]Walter Reed Army Medical Center, Department of Surgery, Washington, DC 20307

Abstract. A reflective, pulsed terahertz (THz) imaging system was used to acquire high-resolution ($d_{10-90}/\lambda \sim 1.925$) images of deep, partial thickness burns in a live rat. The rat's abdomen was burned with a brass brand heated to $\sim$220°C and pressed against the skin with contact pressure for $\sim$10 sec. The burn injury was imaged beneath a Mylar window every 15 to 30 min for up to 7 h. Initial images display an increase in local water concentration of the burned skin as evidenced by a marked increase in THz reflectivity, and this likely correlates to the post-injury inflammatory response. After $\sim$1 h the area of increased reflectivity consolidated to the region of skin that had direct contact with the brand. Additionally, a low reflecting ring of tissue could be observed surrounding the highly reflective burned tissue. We hypothesize that these regions of increased and decreased reflectivity correlate to the zones of coagulation and stasis that are the classic foundation of burn wound histopathology. While further investigations are necessary to confirm this hypothesis, if true, it likely represents the first in vivo THz images of these pathologic zones and may represent a significant step forward in clinical application of THz technology. © 2012 Society of Photo-Optical Instrumentation Engineers (SPIE). [DOI: 10.1117/1.JBO.17.4.040503]

Terahertz (THz) illumination includes the millimeter and submillimeter-wavelength (3 to 0.033 mm) bands of the electromagnetic spectrum with frequencies between 100 GHz and 10 THz. The last decade has witnessed significant proliferation of THz devices, technologies, and applications with considerable attention given to medical imaging and diagnostics.[1] THz medical imaging has been applied to the detection and spatial mapping of skin cancer,[2] corneal hydration,[3] and breast cancer.[4] Recently, THz imaging has been successfully applied to the imaging of burn wounds on ex vivo pig.[5] Furthermore, THz point spectroscopy was recently reported on in vivo rat burn models.[6] These results detected local hydration changes due to burn temperatures and have demonstrated possible clinical applications of THz burn imaging.

This paper builds upon our earlier ex vivo work[5–7] and presents the first known THz imagery acquired of burn wounds in vivo. The results were obtained on an anesthetized rat model with a deep partial thickness burn induced by a heated brand using a previously established protocol.[8] The burn wound was illuminated with 525 GHz in reflection at a 14 deg incidence angle, and a spot size of 1.1 mm (details of the system used to acquire the images in this manuscript can be found here). Images were acquired every 15 to 30 min for over 7 h. During the 7-h study, edema was observed to form in and around the wound and then localize to just the burned area as captured in the THz images. Additionally, an area of hypoperfused tissue formed around the burn area was observed, and it is speculated that this is the zone of stasis: a zone demarking viable and unviable skin.

The study was approved by the UCLA Institutional Review Board (#2009-094-02). One male Sprague Dawley rat weighing 200 to 300 g was purchased from Harlan laboratories, Hayward, CA. Isofluorane anesthetic was used at 4% for induction and 1.5% for maintenance. Prior to burning, the animal was subcutaneously injected with buprenorphine (an analgesic, 0.05 mg/kg). Both of these drugs and their corresponding delivery methods were chosen to minimize any physiological activity that would affect/confound the rat's immune response to the burn. A flat $\sim$4 $\times$ 4 cm^2 area on the lower abdomen was selected and shaved to allow maximum skin exposure [Fig. 1(a)]. The rat was then placed on its back on a Plexiglas mount and its arms and legs secured to the Plexiglas with tape. A nose cone connected to the 1.5% isofluorane induction was placed over the snout and left for the remainder of the experiment.

A 12.7 m thick Mylar window suspended from a steel frame was placed over the shaved area pressed against the abdomen with contact pressure for imaging. An image of the rat mounted in the system is shown in Fig. 2. A 35 $\times$ 35 mm^2 scan of the windowed abdomen skin was taken prior to injury. Following this, a burn was inflicted using a brass brand in the shape of a "+" (20 $\times$ 20 $\times$ 20 mm^3) within the control scan area where the "+" measures 20 $\times$ 20 mm^2 and each "arm" is $\sim$2.5 mm wide. The brand was heated to 220°C using a hot plate to induce a deep partial thickness burn as confirmed by visual inspection and histology. The brand was applied to the abdomen skin with contact pressure for $\sim$10 sec. The animal was then scanned every 15 min for the first hour and every 30 min afterward for a total of 7 h, taking less than 8 min to acquire an image.

The Mylar window was removed between each image acquisition to allow the burn injury response to progress normally. The burn was monitored superficially throughout the experiment and did not display any change in appearance, geometry, color, etc. Furthermore, the injury did not blister. An image of the burn immediately following the application of the brand is shown in Fig. 1(b).

Figure 2 shows the experimental set up and the THz image of the unburned skin beneath the Mylar window is displayed in Fig. 3(a). The white circular field of view (FOV) is a
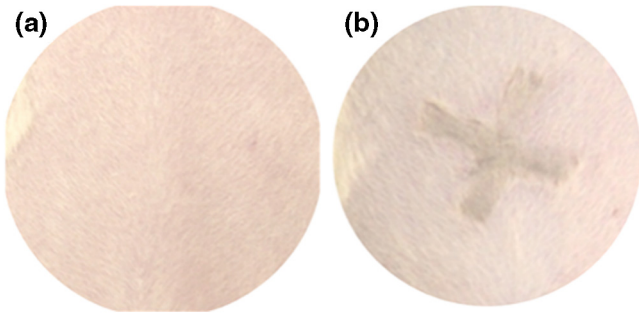
Fig. 1 Abdomen skin: (a) uninjured belly skin prior to application of burn; (b) "+" branded rat abdomen skin after ~7 h.
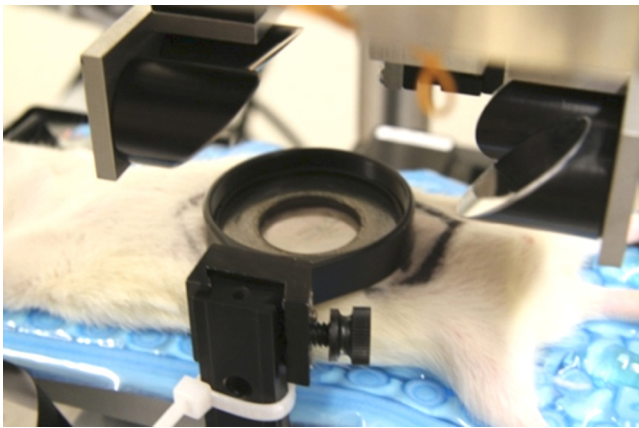

Fig. 2 Rat sample mounted beneath the imaging system. The blue region of the image is the hot water pad used to maintain the rat's normal body temperature (37°C).

Fig. 3 THz images of rat skin burn. The lighter areas correspond to areas of higher reflected signal, and the digits at the bottom left correspond to the elapsed time following the burn. Color bars report the approximate change in water concentration as computed from the measured THz reflectivity and a recently reported skin model. (a) Uninjured skin; (b) 10 min post burn; (c) >1 h; (d) >7 h.

consequence of the metal mounting of the Mylar window. The Mylar is thick enough to flatten the field but still sufficiently thin to conform to the skin surface roughness. This surface roughness is responsible for the small variation across the field and displays an average reflectivity of 5% and a coefficient of variance of 0.022. A THz image 10 min following the burn is displayed in Fig. 3(b). It is known that the post-injury response is characterized by an inrush of edema (majority water).[9] Additionally, our previous work has shown that THz imaging is extremely sensitive to changes in the local water concentration in skin (and has been demonstrated in a number of phantom characterization targets).[3,5,7] Therefore, burn wounds are ideally suited for THz imaging applications as they cover a relatively large area of skin and are known to provoke an extreme post-injury response. This response is apparent in the image Fig. 3(b). It can be seen that both the directly burned skin and surrounding areas display significantly increased THz reflectivity displayed, likely representing an increase in local water concentration that is a normal part of post-injury response. The brand shape is not quite discernable at this time point, and the field displays an average THz reflectivity of ~9.4%; a 4.4% increase from unburned skin. In Fig. 3(c) the edematous response has begun to organize and the shape of the brand is now visible. Furthermore, a dark, low reflecting border has formed around the perimeter of the burn injury. At ~7 h [Fig. 3(d)] the response has fully organized, and the edema is localized to the contact area with an average reflectivity of 9.3%. The surrounding tissue has returned to normal reflectivity. Further inspection of the THz
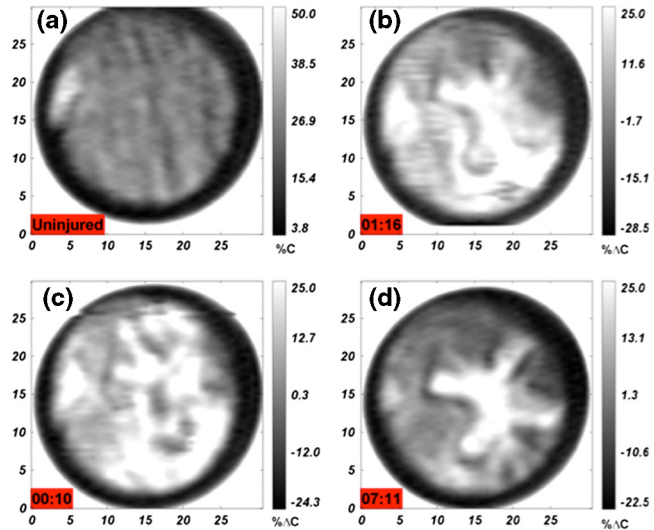
image confirms that the hypoperfused area now encircles the entire burn wound. The color bars in Fig. 3 report the approximate change in water concentration as computed from the measured THz reflectivity and a recently reported skin model.[10] In this model the skin is assumed a homogenous medium consisting of a mixture of collagen water with experimentally measured dielectric functions.[10] The volume fraction of water to collagen required to yield the observed reflectivity was then computed. The pixels displayed Fig. 3(a) were then mapped from reflectivity values to estimated hydration. Figure 3(b) and 3(d) report changes in concentration with respect to the observed mean in Fig. 3(a) and were calculated using the same effective medium theory model.

Classic burn wound pathophysiology describes three concentric wound regions: the zones of coagulation, stasis, and hyperemia.[11] The zone of coagulation is at the center of the burn and contains irreversibly damaged cells, denatured protein, and edematous (hyperhydrated) tissue. The zone of stasis surrounds the zone of coagulation and contains hypoperfused (dehydrated) tissue. The zone of hyperemia forms the outer ring and is characterized by edematous, hyperperfused tissues. Concomitant with the appearance of these three zones are large fluid shifts both locally and systemically. Investigations into these fluid shifts have concluded that local water concentration can increase by as much as 80% within 10 min of injury, and that this response is proportional to the depth of injury.[9,12]

Given the large shifts in location and intensity of the observed THz reflectivity, we believe that we are observing the formation and evolution of the zone of coagulation (high reflectivity center of the burn) and zone of stasis (ring of low reflecting tissue surrounding the highly reflective center). Figure 4 displays a cut through the upper right arm of the "+" brand and confirms a significant increase in reflectivity (hydration) in the burn wound center and a significant drop in skin reflectivity (denoted by the black arrows) in the surrounding tissue. The zone of coagulation displays an increase in hydration of >20% with respect to the uninjured skin
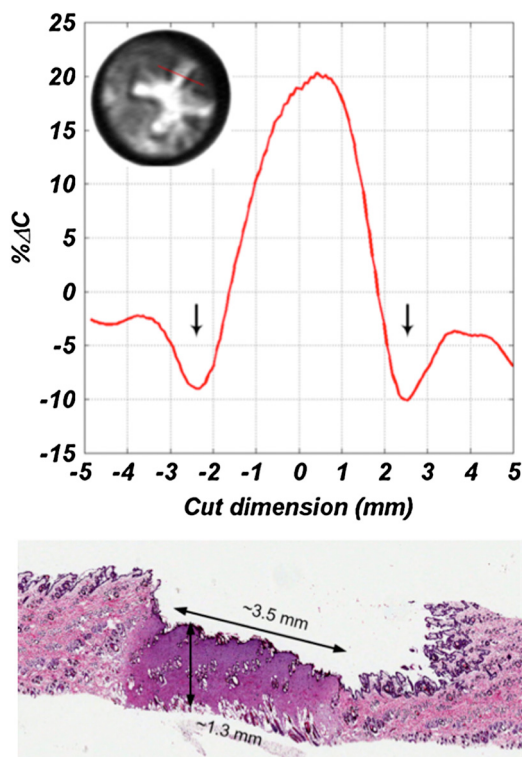
Fig. 4 Top: Cut through one of the arms of the "+" burn showing the dips in reflected signal corresponding to the zone of stasis. The zone of coagulation displays an increase in hydration of >20% with respect to the uninjured skin, while the zone of stasis displays a drop in hydration of up to ~10%. Bottom: A scan of one of the H&E stained sections spanning the burned and surrounding unburned region denoted by the red line in top figure.

while the zone of stasis displays a drop in hydration of up to ~10%. To our knowledge this is the first time that the zone of stasis has been imaged *in vivo* with any imaging technology. Companion histological analysis from a section collected in the region denoted by the red line in the top of Fig. 4 was performed, and a scan of one of the slides used for diagnosis is displayed beneath the image cut. The section spans the burned and surrounding unburned region across the arm and suggests the damage is limited to the dermal layer. Evaluation by a staff pathologist confirmed a deep partial thickness injury. Further studies are underway to correlate the existence and shape of the different zones with burn wound severity.

In conclusion we have presented THz imagery of burn wounds *in vivo*. The images display the formation and dissipation of edema in and around the burn injury. Further, these imaging results may have identified the zones of coagulation and stasis based on high-resolution maps of hydration gradients. The inner zone of coagulation was represented by an area of hyper-reflectivity correlating to the area of most severe injury. The zone of stasis was seen as a low-reflecting region around the perimeter of the burn injury. These zones are visible as early as 1-h post burn, which may offer predictive capabilities superior to that of photoacoustic, laser Doppler imaging (LDI),

and thermal imaging. This is a promising result for THz medical imaging as no other imaging technology has been able to differentiate these regions with such high contrast.[13–16]

Clinicians caring for burns must balance competing interests; restoring intravascular volume to prevent systemic shock while simultaneously minimizing excess fluid administration to prevent burn wound progression and loss of potentially viable tissue. Early identification and monitoring of zone of stasis in severe burns can help guide the surgical excision process resulting in faster healing and minimum scarring thereby reducing the time and cost of treatment. Given the high sensitivity to water concentration and relative robustness to surface scatter and other confounding factors, THz imaging may be able to delineate between different wound zones and help differentiate between viable and unviable tissue.

References

1. P. Siegel, "Terahertz technology in biology and medicine," *IEEE Trans. Microw. Theor. Tech.* **52**(10), 2438–2447 (2004).
2. R. M. Woodward et al., "Terahertz pulsed imaging of skin cancer in the time and frequency domain," *J. Biol. Phys.* **29**(2–3), 257–261 (2003).
3. D. B. Bennett et al., "Terahertz sensing in cornal tissues," *J. Biomed. Optic.* **16**(5), 057003 (2010).
4. A. J. Fitzgerald et al., "Terahertz pulsed imaging of human breast tumors," *Radiology* **239**(2), 533–540 (2006).
5. Z. D. Taylor et al., "Reflective THz imaging of porcine skin burns," *Optic. Lett.* **33**(11), 1258–1260 (2008).
6. M. H. Arbab et al., "Characterization of burn injuries using terahertz time-domain spectroscopy," *Proc. SPIE* **7890**, 78900Q (2011).
7. Z. D. Taylor et al., "THz imaging based on water-concentration contrast," *Proc. SPIE* **6949**, 69490D (2008).
8. F. C. Regas and H. Ehrlich, "Elucidating the vascular response to burns with a new rat model," *J. Trauma* **32**(5), 557–563 (1992).
9. E. Reiss et al., "Fluid and electrolyte balance in burns," *J. Am. Med. Assoc.* **152**(14), 1309–1313 (1953).
10. D. B. Bennett et al., "Stratified media model for terahertz reflectometry of the skin," *IEEE Sensor. J.* **11**(5), 1253–1262 (2011).
11. D. Jackson, "The diagnosis of the depth of burning," *Br. J. Surg.* **40**(164), 588–596 (1953).
12. G. Warden, "Burn shock resuscitation," *World J. Surg.* **16**(1), 16–23 (1992).
13. H. F. Zhang, K. Maslov, and L. Wang, "Imaging acute thermal burns by photoacoustic microscopy," *J Biomed. Optic.* **11**(5), 054033 (2006).
14. M. Yamazaki et al., "Measurement of burn depths in rats using multiwavelength photoacoustic depth profiling," *J. Biomed. Optic.* **10**(6), 064011 (2005).
15. M. Kaiser et al., "Noninvasive assessment of burn wound severity using optical technology: a review of current and future modalities," *Burns* **37**(3), 377–386 (2011).
16. A. D. Jaskille et al., "Critical review of burn depth assessment techniques: part II. Review of laser Doppler technology," *J. Burn Care Res.* **31**(1), 151–157 (2010).